

Hardness of bi-layer films on a leadframe substrate

JANG-KYO KIM*

*Department of Mechanical Engineering, Hong Kong University of Science & Technology, Clear Water Bay, Hong Kong
E-mail: mejkkim@ust.hk*

DO-HYUNG KIM, PYUNG HWANG

School of Mechanical Engineering, Yeungnam University, Gyongsan, 712-749 South Korea

The indentation hardness and elastic modulus of leadframe materials that consist of Cu alloy substrate and Ni/Pd bi-layer films of differing thicknesses are characterised using the micro-hardness and nano-indentation tests. The 'true' hardness of the individual substrate and film layers is evaluated based on the empirical relationship between the measured 'composite' hardness and the volume of plastically deformed material of film layers. It is found that the composite hardness determined from the nano-indentation test increases rapidly toward a peak at extremely low indentation depth of less than about 20–30 μm for all materials studied, due mainly to the finite value of the indenter tip radius and the rough surface of the specimen on the nano-scale. The composite hardness for the coated specimens decreases with further increasing indentation depth toward the hardness value of the substrate, because of the strong influence of the film/substrate interaction and the indentation size effect. The nano-indentation test in general gives higher true hardness values than those obtained from the micro-hardness test. Nevertheless, the relative hardness values of the substrate and films determined from the two tests are consistent. The hardness of Ni film is about 20 to 50% greater than that of Cu alloy, whereas the hardness of Pd film is 7 to 11 times the Ni film in the nano-indentation test. © 2000 Kluwer Academic Publishers

1. Introduction

A surface finish that is gaining increased popularity for Cu leadframe surface for integrated circuit packaging is the Ni/Pd system. These coatings are designed to ensure good electrical conductivity, wire-bondability, solderability and corrosion resistance against moisture. The thick Ni layer is the undercoat to which the wire and solder ultimately bond. The thin Pd primary layer serves as the protective coating that can provide a surface suitable for wirebonding and soldering as well as withstand the thermal stresses generating during solder reflow and moulding compound encapsulation. As such, an accurate control of the properties and thickness of the individual coatings and the bonding with substrate are essential to the performance of the leadframe, which in turn control the reliability of the whole package system [1].

The mechanical characteristics of coatings or thin films, such as hardness and elastic modulus, are very difficult to measure due to the predominant effect of the underlying substrate. Micro-indentations normal to the surface of thin film usually results in deformation of both the film and substrate, providing only 'compos-

ite' hardness data. The composite hardness is a complex function of materials and geometric factors, such as the properties of the film and substrate, the ratio of indentation depth to the film thickness, h/t_f , and the indenter tip geometry [2, 3]. The interface characteristics and the friction between the indenter and film are also important in determining the composite hardness. To obtain a 'true' hardness value of a thin film, which is independent of the substrate, it is necessary for the ratio, h/t_f , to exceed a critical value so that the subsurface deformation beneath an indenter is not influenced by the proximity of interfaces or free surfaces [4]. The critical value varies between about 0.07 and 0.2 depending on the relative hardness values of the substrate and film, the indentation load applied and the indenter tip geometry [5]. The hardness of a thin film determined at very low loads and at indentation depths lying in the range of 0.1–1 μm is much higher than that obtained from the bulk material. For example, for a soft film deposited on a hard substrate such as Ti-coated sapphire [6], the hardness of the Ti film was shown to increase with decreasing film thickness due to enhanced interactions between the film and substrate for the thinner

* Author to whom all correspondence should be addressed.

films. Furthermore, hardness is not a material constant, but varies with load: for most materials, hardness increases with decreasing load [7].

There are various methods to measure the film hardness based on the ‘composite’ hardness data that are obtained from indentations on a coated substrate in a wide range of applied loads. Many attempts have been made to apportion the contributions to the composite hardness from both the film and substrate using a variety of empirical and semi-empirical approaches [4–6, 8] and finite element analyses [6, 9, 10]. A brief review of these studies is presented in the following section. However, little has been reported regarding indentation hardness measurements of multi-layer thin films on a substrate. The purpose of the present study is thus to measure the hardness of Ni and Pd coatings of varying thicknesses on a Cu leadframe substrate. Two different indentation tests, namely the Vicker’s micro-hardness test and the nano-indentation test, are used to evaluate the mechanical interactions between the bi-layer films and the substrate. The results obtained from the two indentation techniques are compared along with discussions of the mechanisms of hardness variation with indentation depth and applied load.

2. Analysis

Due to the wide applications of indentation tests, many theoretical treatments dealing with indentation deformations of films and substrates have been reported to derive expressions or algorithms that relate thin film hardness. In the early work [5], composite hardness, H_c , was given by:

$$H_c = H_s + \alpha(H_f - H_s) \quad (1)$$

where H_f and H_s are the hardness of film and substrate, respectively. α is an empirically derived parameter, which varies with the ratio, h/t_f . Equation 1 looks fundamentally very similar to the expression proposed more recently based on the finite element analysis of elastic and plastic deformation associated with indentation by a conical indenter [10, 11]. The composite hardness, H_c , was expressed as a function of H_f and H_s :

$$H_c = H_s + (H_f - H_s) \exp\left[-\frac{(H_f/H_s)(h/t_f)}{(\sigma_f/\sigma_s)(E_f/E_s)^{1/2}}\right] \quad (2)$$

for a hard film on a soft substrate. σ and E are the yield strength and elastic modulus, respectively; and the subscripts f and s refer to film and substrate, respectively. In Equation 2, Poisson ratio was not specifically considered because it had a negligible effect on ‘composite’ hardness [10]. The mechanical properties of the film and substrate, including σ_f , σ_s , E_f and E_s , should be determined from an independent indentation experiment to evaluate the film hardness.

It was also suggested [12] that the composite hardness was determined by a weighted average of the volume of plastically deformed material in the film, V_f , and in the substrate, V_s . Taking into account the effects

of indentation size and the film/substrate adhesion, the composite hardness was written [4]:

$$H_c = \frac{H_f V_f + H_s V_s \chi^3}{V} \quad (3)$$

where $V (=V_f + V_s)$ is the total volume of material plastically deformed under indentation. χ is an interface parameter that varies with the mismatch between the effective plastic zone radii of film and substrate. The above volume fraction model has been widely used to determine film hardness from the composite response of film and substrate, in particular using the nano-indentation test [6, 13]. In an approach similar to the volume fraction model, the weighted average of the projected areas of the film and substrate, A_f and A_s , on which the indentation pressure acts was also used to express composite hardness [8]:

$$H_c = \frac{H_f A_f + H_s A_s}{A} \quad (4)$$

where $A (=A_f + A_s)$ is the total projected area of the indenter. The surface friction and the interface strength were also incorporated in Equation 4 in a more recent study [14]. Based on the microscopic study of the shape of cracks formed at the Vicker’s indentation rim, Equation 4 was expressed [8, 15] as a function of the ratio of film thickness to indentation depth, t_f/h :

$$H_c = H_s + (H_f - H_s) \left[2C \left(\frac{t_f}{h} \right) - C^2 \left(\frac{t_f}{h} \right)^2 \right] \quad (5)$$

where C is a coefficient that varies with the mode of deformation in the film and the indenter tip geometry. For practical purposes, the value of C was restricted to $0.5 \leq C \leq 1.0$ for the Vicker’s pyramid indenter [15]. Meanwhile, a simple empirical model [8, 15] was also proposed based on the linear relationship that exists between hardness and the inverse of indentation diagonal, d , for indentations larger than a critical size. The hardness for both coated and uncoated substrates, $H(d)$, was given by:

$$H(d) = \frac{k}{d} + H_s \quad (6)$$

where k is the hardness coefficient that is essentially the same as the slope of $H(d)$ versus $1/d$ plot. Therefore, neglecting the second order terms in Equation 5 and rearrangement of Equation 6 gave the expression for film hardness, H_f [8]:

$$H_f = \frac{(k_c - k_s)}{2C t_f} + H_s \quad (7)$$

where $\Delta k = (k_c - k_s)$ is the difference between the coefficients for coated and bare substrates. Equations 5 to 7 are further extended in the present study to apply for bi-layer films on a substrate. The volume of each film deformed under the indenter is assumed approximately

proportional to the thickness of each layer. Thus, the film hardness, H_f , is given:

$$H_f = H_A \frac{t_A}{t_f} + H_B \frac{t_B}{t_f} \quad (8)$$

where t_A and t_B are the thicknesses of films A and B, respectively. Once the hardness of the film A, H_A , is known from an independent experiment on specimens containing a single layer film, the hardness of film B, H_B , can be determined.

3. Experiments

The leadframe materials (supplied by QPL Limited, Hong Kong) consisted of Cu alloy 194 (containing 2.35% Fe, 0.03% P and 0.12% Zn) substrate and deposited Ni/Pd films. Four different combinations of coating/substrate were studied: bare Cu alloy substrate (Specimen 1); 1.48 μm thick Ni coating on the substrate (Specimen 2: 1.48Ni/Cu:); 1.75 μm thick Ni underlayer plus 0.19 μm thick Pd primary finish on the substrate (Specimen 3: 0.19Pd/1.75Ni/Cu); 1.07 μm thick Ni underlayer plus 0.31 μm thick Pd primary finish on the substrate (Specimen 4: 0.31Pd/1.07Ni/Cu). The film thickness was measured to an accuracy of 0.01 μm from the metallographically prepared specimen cross-sections using a precision measuring table equipped with a high magnification optical microscope. Specimens of approximately 5 mm \times 5 mm square cut from the leadframe were used for both the micro-hardness and nano-indentation tests.

Micro-hardness tests were conducted on a Vickers micro-hardness tester (MHT-4 Zeiss micro-hardness tester). Varying indentation loads in the range of 10 and 150 gf (1 gf = 9.807×10^{-3} N) were applied for a constant holding time of 10 s. The indentation diagonal was measured using an optical microscope: a minimum of five readings were made of the indentation diagonals for each set of conditions, and the average diagonal values were used for hardness calculations. Nano-indentation tests were performed on an indenter ('Nano Indenter II' by Nano Instrument Inc.). The indenter consists of an indenter head, an optical microscope connected to a video camera for indentation positioning, and a motorised three-dimensional precision table for transportation of the specimen between the microscope and the indenter. The indenter has a vertical displacement resolution of 0.04 nm and a load resolution of 50 nN. The indenter head is equipped with a three-sided pyramidal diamond Berkovich tip having a tip radius less than 50 nm. The 'continuous stiffness' method was employed to apply continuously increasing loads at a constant loading rate of 10 nm/s to a maximum indenter tip displacement of 1000 nm. The output response provided a series of stiffness and contact area data without discrete unloading cycle. The use of this option eliminated the need for the assumption of contact depth/total depth ratio to determine hardness and elastic modulus as a function of indenter depth [16]. The hardness, H , and reduced elastic modulus, E , taking into account the effect of non-rigid indenter column,

were determined from the equations [16]:

$$H = \frac{P}{A} \quad (9)$$

$$E = \frac{\sqrt{\pi}}{2\beta} \frac{S}{\sqrt{A}} \quad (10)$$

where P is the load, A the contact area, β the geometric constant (≈ 1.034 for a triangular indenter), and S the unloading stiffness.

4. Results and discussion

4.1. Micro-hardness test

Fig. 1 shows the variations of micro-hardness of coated and bare substrates as a function of applied load and indentation depth. One datum point in these figures represents an average of four readings on an indent.

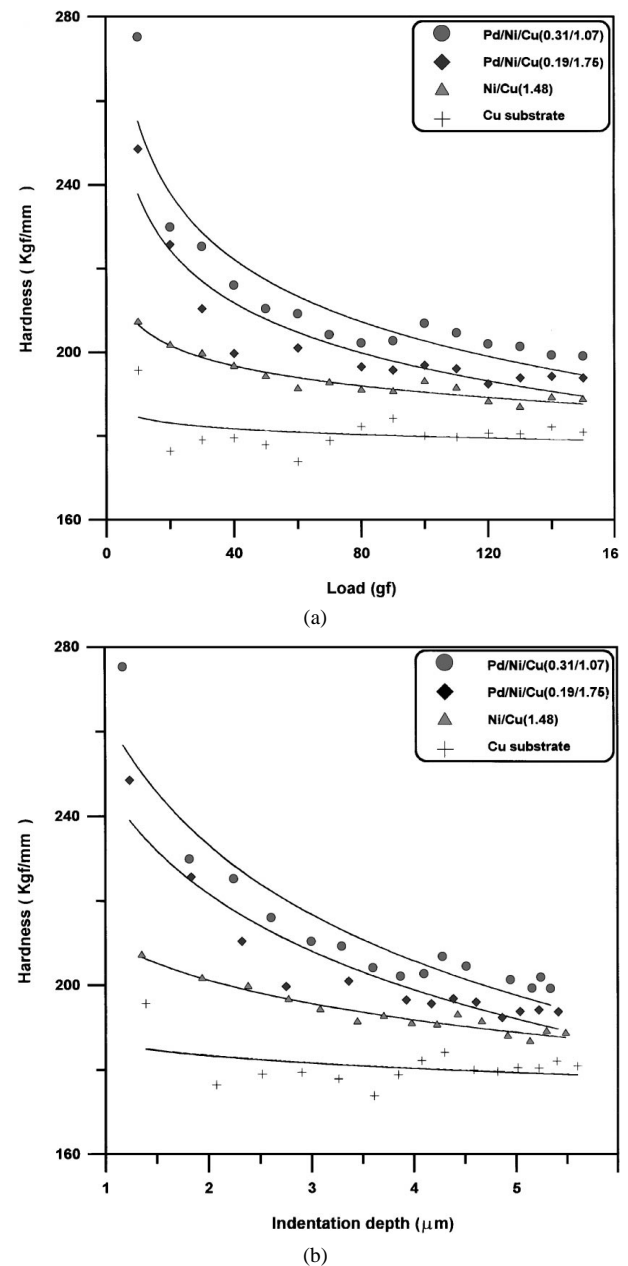


Figure 1 Plots of micro-hardness data as a function of (a) applied load and (b) indentation depth.

The solid lines are non-linear curve fits, showing the general trends. The hardness values for bare copper were almost constant regardless of the load applied, although there was some data scattering between 170 and 190 kgf/mm². The data scattering was probably attributed to the errors arising from incorrect measurements of diagonals of tiny indentations using an optical microscope, especially those obtained at low loads or indentation depths [17]. The micro-hardness data for all coated specimens exhibited a similar trend with respect to indentation load or depth, with strong dependence on the individual hardness and thickness of the films. The hardness decreased parabolically as the indentation depth increased, and converged to a lower plateau value at high indentation depths, due to the film/substrate interaction. The thicker was the hard Pd film, the steeper was the rate of decrease. Comparison of the results between Specimens 3 and 4 containing Pd and Ni films of different thicknesses indicated strong dependence of composite hardness on the film thickness and that the Pd film was much harder than the underlying Ni film, while the Ni film was harder than the Cu alloy substrate. It is not clear why there are moderate increases in hardness for some coated specimens at a load of about 100 gf.

The composite hardness data indeed showed approximately a linear relationship with the inverse of indentation diagonal, $1/d$, as shown in Fig. 2. The corresponding hardness values (in GPa) for the substrate and the individual films determined based on the least squares lines and Equations 6 to 8 are presented in Table I. The substrate hardness values, H_s , were taken from the points where the least squares lines coincided the abscissa in Fig. 2. It should be highlighted that H_s values were almost identical for all materials, with the average value about 1.75 GPa and the variation less than 4%, proving in part the validity of the analysis given by Equations 6 to 8. The hardness values H_{Pd} determined from the specimens with different film thicknesses var-

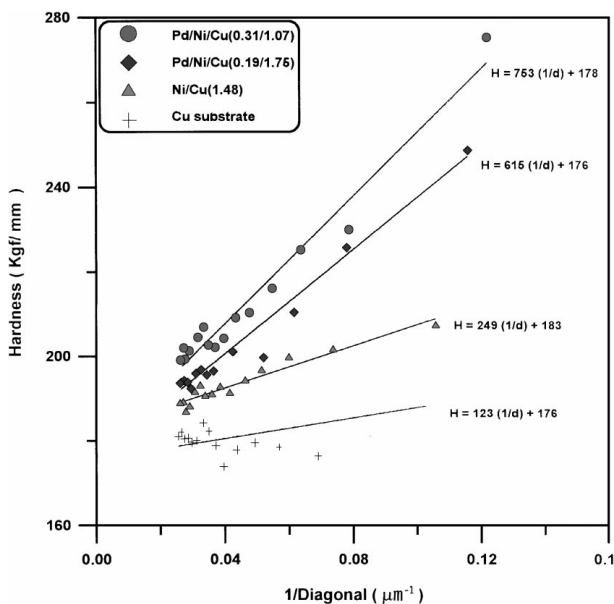


Figure 2 Plots of micro-hardness data as a function of inverse of indentation diagonal, $1/d$.

TABLE I Individual hardness values of Cu alloy substrate, Ni and Pd films that are determined from micro-hardness tests

Specimen	Composition	Hardness (GPa)			
		H_s	H_f	H_{Ni}	H_{Pd}
1	Bare Cu	1.73	-	-	-
2	1.48Ni/Cu	1.79	2.14–2.56	2.14–2.56	-
3	0.19Pd/1.75Ni/Cu	1.73	2.96–4.20	-	10.5–19.3
4	0.31Pd/1.07Ni/Cu	1.74	3.96–6.20	-	10.3–18.8

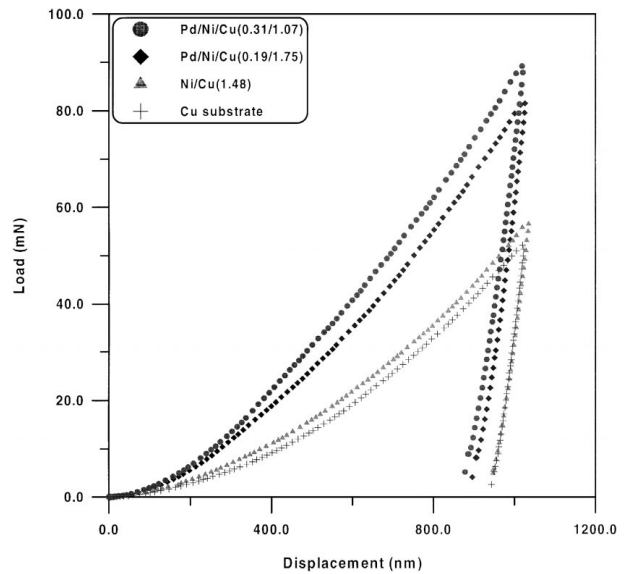


Figure 3 Nano-indentation load versus displacement records.

ied in much the same range. The hardness of Ni film was 22 to 46% greater than that of the Cu alloy, whereas the Pd film hardness was about 5 to 7.5 folds greater than that of the Ni film.

4.2. Nano-indentation test

Fig. 3 presents typical load-displacement records for the four specimens with different film thicknesses that were indented to a maximum depth of 1000 nm. The unloading part of the curves was almost perfectly reversible, indicating that the measurement involved the release of elastic strain under the indenter. It seems clear that the specimens containing a Pd layer required much higher loads than those without one to indent to the same depth, giving rise to high hardness and modulus values. The presence of Ni film on the Cu substrate resulted in only a marginal increase in indentation load compared to the bare Cu. Figs 4 and 5 illustrate variations of composite hardness and elastic modulus of coated and uncoated specimens as a function of applied load and indentation depth, which were obtained from the continuous stiffness test. The composite hardness and elastic modulus displayed essentially a similar trend for very low indentation depths, say less than about 30 nm: these properties increased sharply toward a peak value for all specimens tested, including the bare Cu. The peak value was maintained for a relatively long range of indentation depth for specimens with a Pd film, whilst it was only instantaneous before a steep drop

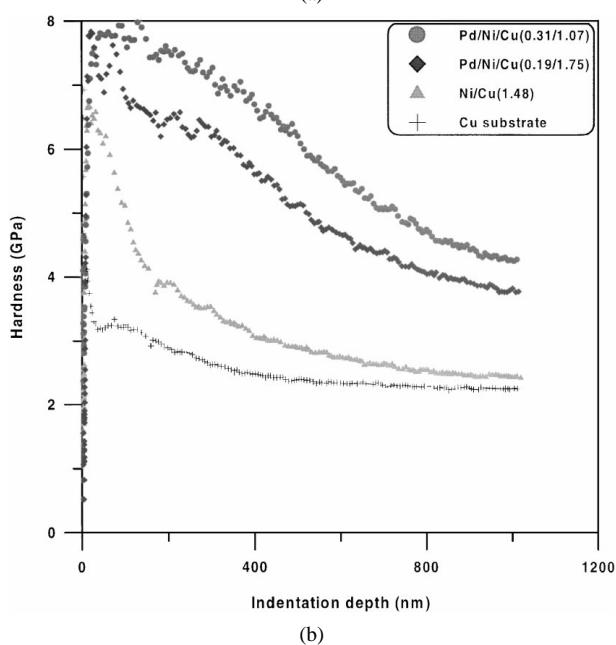
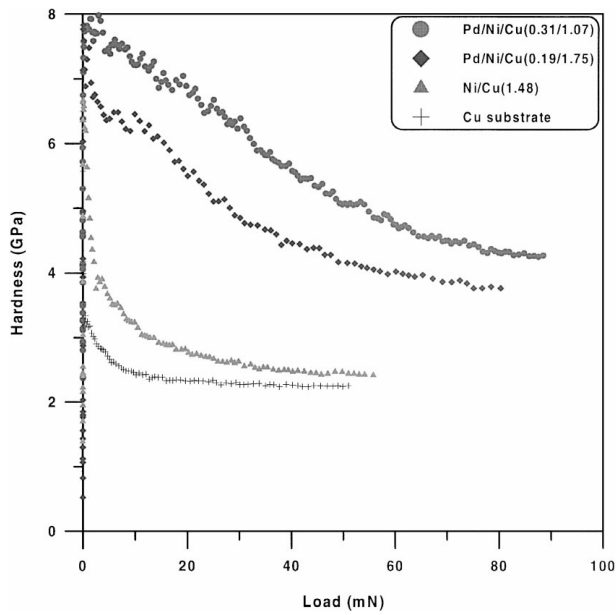


Figure 4 Plots of hardness determined from the nano-indentation test as a function of (a) applied load and (b) indentation depth.

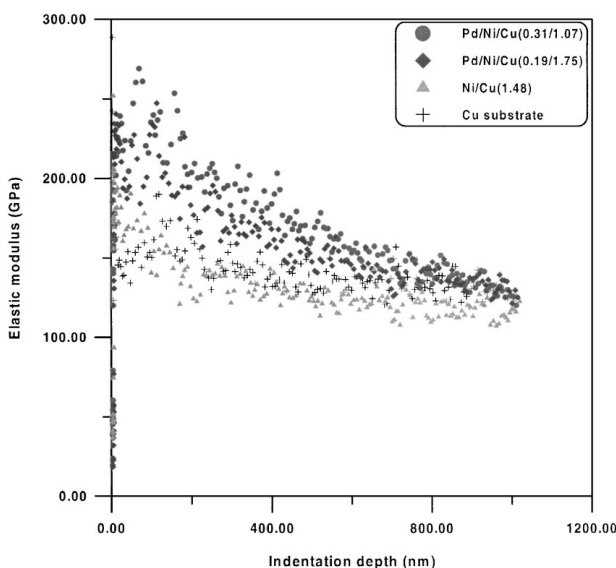


Figure 5 Plots of elastic modulus as a function of indentation depth.

for the bare Cu specimen. It is interesting to note that the indentation depth corresponding to peak composite hardness coincided approximately with 10–20% of Pd film thickness (200–300 nm) for both Specimens 3 and 4. These indentation depths appear to roughly agree with the one-tenth rule [5]-the critical ratio of depth to film thickness-at which the contribution of substrate is almost negligible for a hard film on a soft substrate [18, 19].

The sharply rising initial portion of composite hardness and elastic modulus data needs special accounts. Judging from the fact that this observation was absent in the micro-hardness data, it appears that this observation is a reflection of the artifact arising from finite value of the indenter tip radius and rough surface of the specimen on the nano-scale. The indenter tip radius was known to be less than 50 nm, which is still large enough to cause the calculated projected area or indentation depth to be inaccurate for such shallow indentations. Furthermore, the atomic force microscopic images given in Fig. 6 clearly demonstrate that the surface roughness was as large as a few hundred nanometers for all specimens studied. This suggests strong possibilities of incomplete contact of the indenter tip with the specimen surface during indentation, resulting in erroneous calculations of hardness and elastic modulus for very shallow indentations. For the foregoing reasons, the rising portions of the composite hardness data were not taken into account in determining the individual hardness values of the substrate and films in Fig. 7.

A careful examination of Fig. 4 indicates that the rate of hardness decrease after the peak values depended largely on the type and thickness of films. For specimens with a Pd film, the hardness decreased rather gradually, while for the bare Cu and the Ni coated Cu, the drop after the instantaneous peak was rapid. Therefore, the hardness for bare Cu became almost a constant value of about 2.3 GPa when the indentation depth reached 600 nm, while the composite hardness values for coated specimens were still decreasing even after 1000 nm. Further indentation beyond 1000 nm indicates that the composite hardness for the Ni coated specimen became constant at an indentation depth of about 1500 nm. This is the depth at which the effect of hard film became completely negligible, and the hardness was wholly given by the substrate. However, the hardness for the Pd coated specimens never reached a plateau constant even after an indentation of 3500 nm, suggesting the hard Pd film dictated the whole indentation behaviour in the range of indentation depths studied. Apart from the effect of the softer substrate than the film, the size effect was in part responsible for the decrease in hardness with increasing indentation depth. Since the geometry of an indent is independent of its size, the hardness should, in principle, be independent of applied load. In practice, however, there is a significant dependence on load or indentation depth for crystalline materials [20], which is attributed to a few factors. Dislocations and grain boundaries occur only at limited local densities in very small deformed volumes [21]. The other factor is that the indenter tip is not perfectly formed to comply with geometric assumption

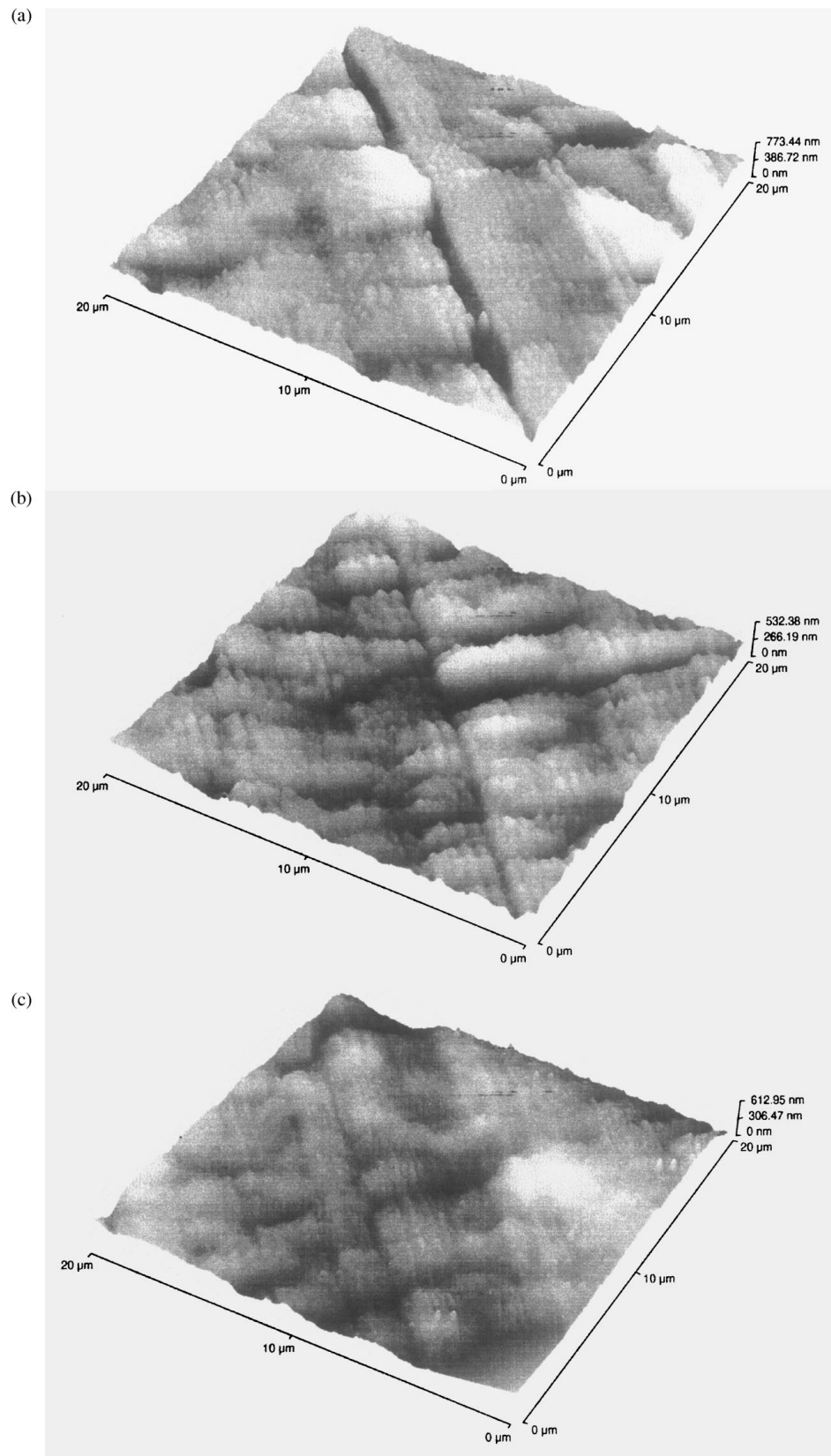


Figure 6 Atomic force microscope photographs of surface morphology for (a) bare Cu alloy, (b) Ni film and (c) Pd film.

on the nano-scale. The non-zero radius of the indenter tip causes the contact to become not fully plastic at low loads [22].

In sharp contrast to the composite hardness data, the elastic modulus for all specimens reached an almost constant value at an indentation of about 1000 nm, indicating less sensitive indentation size effect on elas-

tic modulus. It is noted that the elastic modulus of Cu alloy, 127 GPa, obtained from the present nano-indentation test was quite comparable to the reported value of 118 GPa in the literature [23].

The nano-indentation hardness results were analysed based on Equations 6 to 8 with appropriate modifications to properly account for the different indenter tip

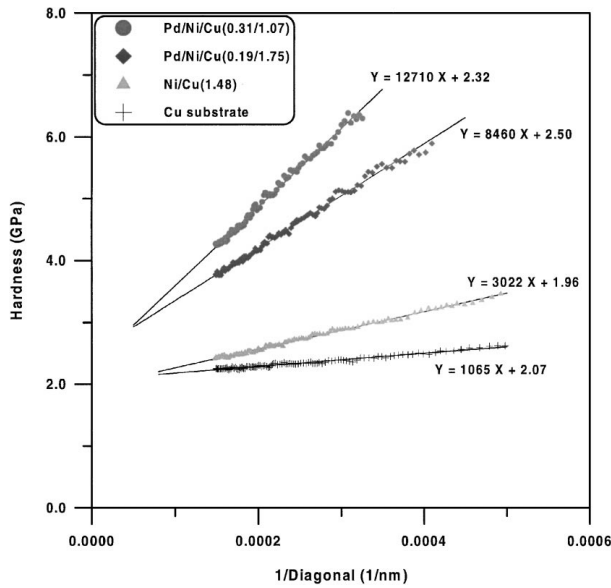


Figure 7 Plots of hardness determined from the nano-indentation test as a function of inverse of indentation diagonal, $1/d$.

geometry. The diagonal, d , was calculated based on the relationship with the indentation depth, h :

$$d = h(\tan \gamma + \tan \theta) \quad (11)$$

where γ and θ are the angles at the Berkovich indenter tip. Thus, d represents the distance between a point and the facing side in the projected indent area of an equilateral triangular shape. The constant, C , in Equation 7 was also modified accordingly for the Berkovich tip, which has a larger tip angle than the Vicker's tip: $0.44 \leq C \leq 0.85$. Fig. 7 shows the least squares plots of the composite hardness as a function of $1/d$ for four different specimens, exhibiting perfectly linear relationships. The corresponding hardness values of the substrate and individual films are summarised in Table II. The nano-indentation test produced generally higher hardness values for all materials tested than those obtained from the conventional micro-hardness test, due to the apparent indentation size effect as explained above [24]. Nevertheless, the relative hardness values between different materials obtained from the two test methods showed a very similar trend: the hardness of Ni film was about 20 to 50% greater than that of Cu alloy, while the Pd film hardness was 7 to 11 times greater than that of Ni film in the nano-indentation test. Further, it should be noted that the hardness of Pd film obtained from two different specimens were almost identical, partly demonstrating the applicability of the empirical

TABLE II Individual hardness values of Cu alloy substrate, Ni and Pd films that are determined from nano-indentation tests

Specimen	Composition	Hardness (GPa)			
		H_s	H_f	H_{Ni}	H_{Pd}
1	Bare Cu	2.07	-	-	-
2	1.48Ni/Cu	1.96	2.74–3.46	2.74–3.46	-
3	0.19Pd/1.75Ni/Cu	2.50	4.74–6.83	-	23.1–37.9
4	0.31Pd/1.07Ni/Cu	2.32	7.28–11.9	-	23.0–41.0

model given by Equations 6 to 8 to the nano-indentation test of coated materials.

5. Concluding remarks

The Vicker's micro-hardness and nano-indentation tests were successfully employed to characterise the indentation hardness and elastic modulus of coated and uncoated leadframe materials, including bare Cu alloy, Ni coated Cu alloy and Ni/Pd bi-layer coated Cu alloy. The composite hardness data obtained from the two test methods showed linear relationships with the inverse of indentation diagonal, allowing determination of the individual hardness values of the substrate and films based on the empirical relationship proposed previously. Major findings are summarised in the following.

1. The composite hardness obtained from the micro-hardness test decreased with increasing indentation depth, the rate of decrease being dependent on the type and thickness of films, due to the influence of the film/substrate interaction.

2. The composite hardness determined from nano-indentation tests increased rapidly toward a peak at extremely low indentation depth of less than about 20–30 μm for all materials tested. This is attributed to the finite value of the indenter tip radius and the rough surface of the specimen on the nano-scale. After the peak, the composite hardness showed a sharp decrease with further indentation for bare Cu alloy and Ni film coated specimens, while the decrease was rather gradual for specimens containing a hard Pd film.

3. The nano-indentation test produced generally higher individual hardness values for the Cu alloy, and Ni and Pd films than those obtained from the conventional micro-hardness test, due most likely to the indentation size effect. Nevertheless, the relative hardness values for all materials determined from the two test methods were quite consistent in qualitative terms, which in turn demonstrates the validity of the empirical equations employed.

4. In contrast to the significant variation of composite hardness data with indentation depth, the elastic modulus reached a constant value at an indentation depth of about 1000 nm, indicating less sensitive size effect.

Acknowledgements

The financial supports by the Research Grant Council (RGC) through the grant HKUST6014/98E, and by the School of Engineering, HKUST through the Area of Excellent Grant, AOE97/98.EG14, are acknowledged. The leadframe materials were supplied by QPL Limited, Hong Kong. DHK was a visiting scholar from Yeungnam University, Korea to Hong Kong University of Science & Technology (HKUST), Hong Kong when this work was performed. Most experiments were carried out with the technical supports of Advanced Engineering Materials Facilities (AEMF) and Materials Characterisation and Preparation Facilities (MCPF) of HKUST. Part of the paper was presented at Fourth Asia-Pacific Symposium on Advances in Engineering

Plasticity and Its Applications, which was held in Seoul, Korea in June 1998.

References

1. P. T. VIANCO, *Circuit World* **25** (1998) 6.
2. D. L. JOSLIN and W. C. OLIVER, *J. Mater. Res.* **5** (1990) 123.
3. K. L. DAHM, W. G. FERGUSON, R. MURAKAMI and P. A. DEARNLEY, *Surface Eng.* **10** (1994) 199.
4. P. J. BURNETT and D. S. RICKERBY, *Thin Solid Films* **148** (1987) 41.
5. H. BÜCKLE, in "The Science of Hardness Testing and its Research Application," edited by J. W. Westbrook and H. Conrad (American Society for Metal, Metals Park, OH, 1973) p. 453.
6. B. D. FABES, W. C. OLIVER, R. A. MCKEE and F. J. WALKER, *J. Mater. Res.* **7** (1992) 3056.
7. J. B. PETHICA, R. HUTCHINGS and W. C. OLIVER, *Phil. Mag. A* **48** (1983) 593.
8. B. JÖNSSON and S. HOGMARK, *Thin Solid Films* **114** (1984) 257.
9. F. E. KENNEDY and F. F. LING, *J. Eng. Mater. Technol.* **95** (1974) 97.
10. A. K. BHATTACHARYA and W. D. NIX, *Int. J. Solids Struct.* **24** (1988) 1287.
11. A. K. BHATTACHARYA, *ibid.* **24** (1988) 881.
12. P. M. SARGENT, ASTM SPT 889, Philadelphia, PA, 1986, p. 160.
13. B. D. FABES and W. C. OLIVER, *Mat. Res. Soc. Symp. Proc.* **188**, 127.
14. W. H. POISL, B. D. FABES and W. C. OLIVER, *ibid.* **308**, 201.
15. O. VINGSBO, S. HOGMARK, B. JÖNSSON and A. INGEMARSSON, ASTM STP 889, Philadelphia, PA, 1986, p. 257.
16. G. M. PHARR and W. C. OLIVER, *MRS Bull.* **7** (1992) 28.
17. D. R. KELLY, C. E. JOHNSON and D. S. LASHMORE, ASTM STP 889, Philadelphia, PA, 1986, p. 186.
18. H. M. POLLOCK, D. MAUGIS and M. BARQUINS, ASTM STP 889, Philadelphia, PA, 1986, p. 47.
19. C. J. LU and D. B. BOGY, *Int. J. Solids Struct.* **32** (1995) 1759.
20. G. P. UPIT and A. VARCHIENYA, "The Science of Hardness testing and Its Research Applications" (American Society of Metals, Metal Park, OH, 1971) p. 135.
21. D. TABOR, *Review of Physics in Technology*, 1, 1970, p. 145.
22. C. J. LU, D. B. BOGY and R. KANEKO, *ASME Trans. J. Tribol.* **116** (1994) 175.
23. R. J. PTACEK and D. E. SCHUDER, in Proc. 5th Ann. Intern. Electronics Packaging Society Conf., Orlando, FL, 1985.
24. M. F. DONER and W. D. NIX, *J. Mater. Res.* **1** (1986) 601.

*Received 23 April 1999
and accepted 6 March 2000*